Improved Beam Confinement in the Modified Betatron with Strong Focusing

C. A. Kapetanakos, L. K. Len,[a] T. Smith, J. Golden,[b] K. Smith,[c] S. J. Marsh,[c] D. Dialetis,[d]
J. Mathew, P. Loschialpo, and J. H. Chang

Plasma Physics Division, Naval Research Laboratory, Washington, D.C. 20375

The lifetime of the circulating electron beam in the Naval Research Laboratory modified betatron has been increased by more than 2 orders of magnitude with the addition of strong focusing windings to the device. The injected beam consistently spirals from the injector to the minor axis and is trapped. The ~0.5-kA trapped electron ring has been accelerated above 10 MeV from the injection energy of 0.5 to 0.6 MeV. The beam acceleration has been confirmed not only by the x-ray attenuation technique but also with the detection of photoneutrons.

PACS numbers: 41.80.Ee, 29.20.Fj

Accelerators that combine high-current capability and high effective accelerating gradient are currently under development in several laboratories.[1-5] These accelerators have two common features, namely, strong focusing that improves their current-carrying capability and recirculation that enhances their effective accelerating gradient.

Among these accelerators is the modified betatron.[6-8] This device is currently under investigation at the University of California, Irvine[2] and also at the Naval Research Laboratory[1] (NRL). In its original form the modified betatron consists of a strong toroidal magnetic field and a time-varying betatron field that is responsible for the acceleration.

Extensive studies of beam capture and confinement in the NRL modified betatron led to the formation of electron rings with circulating current as high as 3 kA and have furnished valuable information on the critical physics issues of the concept. In addition, these studies have shown that over a wide range of parameters the ring lifetime was limited to a few microseconds which is comparable to the magnetic-field diffusion time through the vacuum chamber. Thus, it became apparent from these results that the magnetic-field configuration of the device had to be modified to increase the beam lifetime and thus to achieve acceleration. A decision was made to proceed rapidly with the design, fabrication, and installation of strong focusing windings.

Stellarator[9] (four twisted windings that carry current in alternate directions) and Torsatron[10] (two twisted windings that carry current in the same direction) winding configurations were considered. Both configurations have advantages and shortcomings. The stellarator configuration was finally selected not only because of the small net vertical field and the lower current per winding but also because it is compatible with our contemplated extraction scheme.[11,12]

This paper briefly describes the NRL modified betatron in its latest form and summarizes the most impor-

tant experimental results after the installation of the strong focusing windings. Although experiments were carried out at various background pressures, most of the results reported in this paper were limited to pressures between 2×10^{-6} and 8×10^{-6} Torr. In this pressure range the electron-beam electrical neutralization time by direct collisional ionization of the background gas has been estimated to be between 180 and 45 μsec. Work is in progress to reduce the background pressure by at least an order of magnitude and thus avoid substantial plasma formation over the entire beam lifetime. This is in contrast to the main effort in the Stellatron at Irvine[2] that is focused on the formation of runaway electron beams and therefore the pressure is incidentally high.

Description of the experiment.— (1) External magnetic fields: The NRL modified betatron comprises three different external magnetic fields; the betatron field that is a function of time and is responsible for the acceleration of the electrons, the toroidal magnetic field that varies only slightly during the acceleration of the electron ring, and the strong focusing field that also has a very weak time dependence. The coils that generate these three fields are shown schematically in Fig. 1.

(2) The betatron field: The betatron[13] magnetic field controls mainly the major radius of the gyrating electron ring and is produced by eighteen air-core, circular coils connected in series. Their total inductance is approximately 530 μH. The coils are powered by an 8.64-mF capacitor bank that can be charged up to 17 kV. At full charge, the bank delivers to the coils a peak current of about 45 kA. The current flowing through the coils produces a field that varies sinusoidally with time having a quarter period of 2.5 msec and an amplitude on the minor axis at peak charging voltage equal to 2.1 kG. Immediately after the peak the field is crowbarred with a 4.5-msec decay time.

The flux condition and field index are adjusted by two sets of trimmer coils that are connected in parallel to the main coils. The current through the trimmers is adjust-
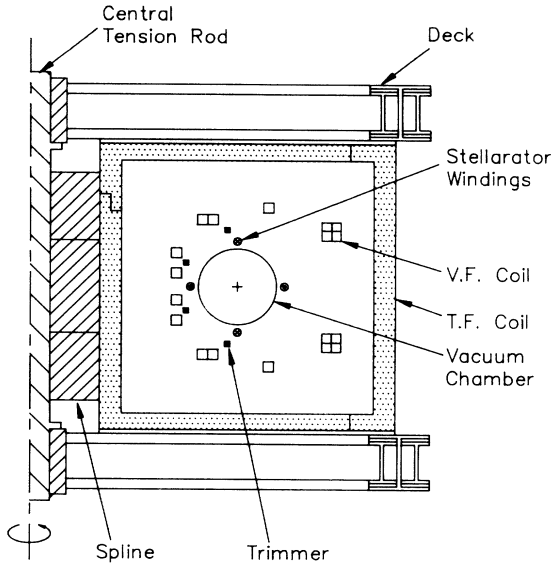
FIG. 1. Elevation of the device showing the vertical field (V.F.), toroidal field (T.F.), stellarator windings, and some structural components.

ed with series inductors. Typically $\sim 10\%$–15% of the total current flows through the trimmers.

(3) The toroidal field: The toroidal magnetic field controls mainly the minor cross section of the electron ring and the growth rate of several unstable collective modes. This field is generated by twelve air-core, rectangular coils that are connected in series.

The coils are made of aluminum square tubing and have a 150 cm height and 135 cm width. The total inductance of the twelve coils is ~ 85 μH and are powered by a 24-mF capacitor bank that can be charged to a peak voltage of 10.6 kV. At peak voltage, the bank delivers to the coils ~ 180 kA. This current produces a field that varies sinusoidally with time having a quarter period of 1.9 msec and an amplitude on the minor axis equal to 3.9 kG.

(4) The strong focusing field: The strong focusing field improves the confining properties of the other two fields by reducing the sensitivity of the beam centroid and individual electrons to energy mismatch and energy spread.

In the NRL modified betatron the strong focusing field is generated by four twisted windings carrying current in alternate directions. The left-handed windings are located 23.4 cm from the minor axis and have a 209.4-cm period, i.e., there are three periods over the circumference of the torus. They are supported by epoxy-reinforced graphite jackets and have been designed to carry up to 25 kA. The windings are connected in series and the current temporal profile is controlled by a ballast inductor.

The stellarator field index n_{st} is defined, in the linear approximation, as[10]

$$n_{st} = -(\Omega_s^{ex}\epsilon_{st})^2 a r_0 / 2\Omega_{z0}\Omega_{\theta 0},$$

where

$$\Omega_s^{ex}\epsilon_{st} \approx 4a\Omega_0\rho_0 K_2'(2a\rho_0),$$

$\Omega_0 = |e|B_0/m$, $B_0 = 2\mu_0 I_{st}/L$, $a = 2\pi/L$, r_0 is the major radius, K_2' is the derivative of the modified Bessel function, and Ω_{z0} and $\Omega_{\theta 0}$ are the cyclotron frequencies of the vertical and toroidal fields on the minor axis. Since in the NRL modified betatron I_{st}, $\Omega_{\theta 0}$, and Ω_{z0}/γ remain approximately constant during acceleration, n_{st} scales inversely proportional to the relativistic factor γ. The stellarator field index is related to the maximum gradient g $[=(\partial B_z/\partial r)_{max}=(\partial B_z/\partial z)_{max}]$ of the stellarator field by $n_{st} = -g^2 r_0/2aB_{z0}B_{\theta 0}$. For $B_{\theta 0}=2.0$ kG, $B_{z0}=25$ G, $a=-0.03$/cm, $\rho_0=23.42$ cm, and $I_{st}=19$ kA, $n_{st}\simeq 14$, and $g\simeq 20$ G/cm.

(5) The vacuum chamber and diode: The 100-cm major radius, 15.2-cm-inside minor radius vacuum chamber has been constructed using epoxy-reinforced carbon fibers. The desired conductivity is obtained by embedding a phosphor bronze screen inside the body of the graphite. The graphite is 2.5 mm thick and has a surface resistivity of 26.6 mΩ on a square. The screen has 250×250 wires per inch and is made of 40-μm-diam wire with an equivalent surface resistivity of 12.8 mΩ on a square. The calculated resistance for the entire vacuum chamber is 57 mΩ. The measured dc resistance of the toroidal vacuum vessel is 68 ± 2 mΩ. The outside surface of the chamber is covered with a 6.3-mm-thick, epoxy-reinforced fiberglass layer.

This novel construction technique has several attractive features, including controllable resistivity and thus magnetic-field penetration time, high stiffness, and tensile strength, high-radiation resistance (up to 500 Mrad) and low-outgassing rate ($\sim 10^{-8}$ Torr/sec cm^2).

The electrons are emitted from a thin carbon disk mounted at one end of a 2.5-cm-diam cylindrical cathode stalk clad with molybdenum. The carbon disk is flush with the molybdenum cladding and faces the circular opening of the conical anode, that is located 8.7 cm from the minor axis of the toroidal chamber. To minimize the magnetic-field component transverse to the emitting surface of the cathode the core of the cathode stalk is made out of high $\sigma\mu$ ferromagnetic material. The unsaturated state of the ferromagnetic material is prolonged by a thin copper housing.

Experimental results.— During the first microsecond following injection, the beam transverse motion is studied by monitoring the light emitted from a 10-μm-thick polycarbonate foil that is stretched across the minor cross section of the vacuum chamber.[1] The foil is graphite coated on the upstream side to avoid electrostatic charging. Figure 2 shows two open-shutter photographs of the light emitted as the ring passes through the foil.
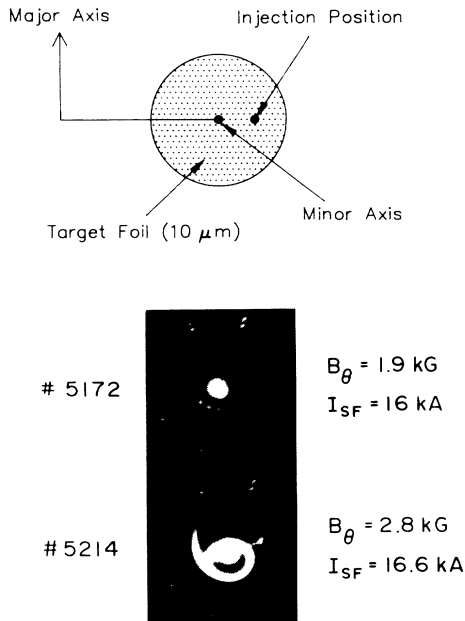
FIG. 2. Open-shutter photographs of the light emitted when the beam passes a 10-μm-thick foil.

The light spots near the edges of the photograph are position fiducials produced by a ring of light-emitting diodes located approximately 0.7 cm from the vacuum chamber wall. Reflections from the wall are also noticeable near the upper edge of the photograph.

For several combinations of injection parameters the beam consistently spirals from the injection position to the minor axis and is trapped. The transit time of the beam to the minor axis is typically less than 0.5 μsec. In shot No. 5172 both the beam current and B_θ are low and thus the bounce frequency is high. As the beam spirals from the diode to the minor axis it creates distinct light spots as it passes through the foil. By increasing the beam current and B_θ the bounce frequency is reduced and thus the light spots start to overlap and the spiral becomes continuous as in shot No. 5214.

The trapping mechanism is presently unknown. A likely candidate is the wall resistivity. However, the predicted decay rate Γ^{-1} from the linear theory[14] for the parameters of the experiment is between 10 and 20 μsec, i.e., too long to explain the experimental results.

The circulating electron ring current is monitored with two Rogowski coils that are located inside the vacuum chamber. A typical wave form is shown in Fig. 3. Although some losses occur immediately after injection, the circulating current remains practically constant during the first 10 μsec. Observations are limited to 10 μsec by the signal level and the 100-μsec passive integrator. Attempts to use active integrators have been, so far, unsuccessful.

In the results reported here the injected electron beam is produced by a diode with a 1-cm-diam carbon cathode
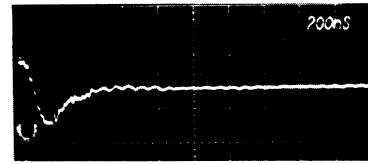

FIG. 3. Output from a Rogowski coil that is located 15° downstream of the diode. The plateau (trapped current) corresponds to 525 A.

disk that is matched to a 1-cm-diam anode hole. For such a beam radius the maximum trapped current is between 0.5 and 0.6 kA. The results indicate that the trapped current increases as the beam diameter increases. Experiments with larger radius beams are presently in progress.

The ring lifetime is inferred from the x rays produced when the beam strikes a 2.5-cm-wide, 1-mm-thick lead limiter. The x rays are monitored by a collimated x-ray detector (scintillator-photomultiplier tube) that is housed inside a lead box. In the results reported in this paper, the x rays enter the scintillator through a 1.94-cm-diam hole and the detector is located 10.8 m from the target. A typical wave form of the x-ray monitor is shown in Fig. 4. From the value of the B_z field it can be easily computed that the main peak of the x-ray signal corresponds to a particle energy near 11.0 MeV. The energy of the electrons that are lost at a later time is obviously higher.

The x-ray signal is very reproducible in both amplitude and shape. For the first 200–300 μsec we do not observe any x rays. The time at which x rays are initially observed and the times the various signal peaks occur are directly proportional to B_θ and inversely proportional to dB_z/dt. In addition, the temporal occurrence of the

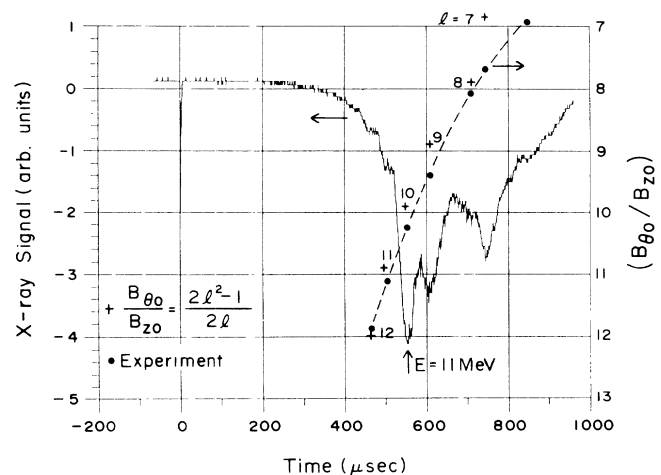
FIG. 4. Output of the x-ray detector vs time and $B_{\theta 0}/B_{z0}$ at the peaks of the x-ray signal for $B_{\theta 0} = 3.6$ kG, $I_{SF} = 20$ kA, and $\langle B_z \rangle / B_{z0} = 1.9$.

x-ray signal appears to be independent of the trapped current for at least up to 0.5 kA and also of the background pressure up to 6×10^{-5} Torr. However, the amplitude of the x-ray signal decreases rapidly with increasing pressure above 8×10^{-6} Torr. For the results of Fig. 4, the electrons gain energy at the rate of 0.39 keV/ revolution. Those electrons lost at the main x-ray peak have performed in excess of 28 000 revolutions around the major axis. In our best results the corresponding number is $\sim 35\,000$ revolutions and the electron energy about 12 MeV.

The spiky shape of the x-ray signal and therefore the beam loss is consistent with the excitation of the cyclotron resonance.[15,16] Figure 4 also shows the ratio B_θ/B_z versus time. The solid circles are from the experiment and the crosses are the prediction of the theory. The poor argument between theory and experiment for low-l values is probably associated with the omission of toroidal effects in the theoretical model. The results are also consistent with the excitation of the electron-cyclotron instability.[17] This instability is caused by the coupling of the electron-cyclotron mode to the TE_{11} waveguide mode of the torus. Work is in progress to pinpoint the exact cause of the beam loss.

The x-ray signal has been studied with the usual attenuation technique. A layer of lead more than 5 cm thick is needed to completely eliminate the signal. A 1.3-cm-thick layer does not have any effect on the signal except on the initial spike that is due to the injected beam. In addition to the x-ray attenuation technique, the beam acceleration has been confirmed with the photoneutrons produced from the $D(\gamma,n)H$ reaction. A plastic tube in the form of a ring containing heavy water was inserted behind the limiter. The photons produced on the target photodisintegrate the deuterium and produce neutrons that are monitored with a rhodium activation detector.[18] The number of counts measured during the first minute exceeds 7 standard deviations.

The intensity and polarization of the synchrotron radiation has been computed numerically. At low energy (≤ 1 MeV) the radiation spectrum is dominated by a peak at the Doppler-shifted B_θ cyclotron frequency. As the electron energy increases the effect of the B_θ cyclotron motion is reduced and the spectrum approaches that of a purely circular orbit.

Two high-gain (50 db) heterodyne receivers are used to monitor the emitted radiation in the bands 26.5–28.5 and 36.5–38.5 GHz during acceleration. The measurements show that the amplitude of the radiation scales linearly with the trapped ring current. During the first 200 nsec, both the amplitude and polarization are consistent with the predicted single-particle emission. In addition, the temporal shift of the first peak is in good agreement with the predicted toroidal field and energy dependence of the Doppler-shifted cyclotron frequency. However, the late-time behavior of the radiation signals is not presently well understood. The radiation signal starts to decay after ~ 200 μsec, contrary to the prediction of the theory. It is likely that electron losses, plasma formation, or beam displacement out of the field of view of the detectors are responsible for the observed discrepancy.

Note added.—Since the submission of the paper, the trapped current increased to 0.9–1.0 kA and the beam energy to 15–16 MeV.

---

[a]Permanent address: FM Technologies, Inc., 10529-B Braddock Road, Fairfax, VA 22032.

[b]Permanent address: Berkeley Research Associates, 5532 Hempstead Way, Spring Field, VA 22151.

[c]Permanent address: Sachs/Freeman Associates, Inc., Landover, MD 20785.

[d]Permanent address: Science Applications, Inc., 1710 Goodridge Drive, McLean, VA 22102.

[1]J. Golden et al., in Proceedings of the Seventh International Conference on High-Power Particle Beams, Karlsruhe, Germany, July 1988, edited by W. Bauer and W. Schmidt (Kernforschungszentrum Karlsruhe GmbH, Karlsruhe, 1988), Vol. I, p. 221.

[2]H. Ishizuka et al., in Proceedings of the Seventh International Conference on High-Power Particle Beams (Ref. 1), Vol. II, p. 857.

[3]S. Humphries, Jr., and L. K. Len, in Proceedings of the 1987 Particle Accelerator Conference, Washington, DC, March 1987, edited by E. R. Lindstrom and L. S. Taylor (IEEE, New York, 1987), p. 914.

[4]V. Bailey et al., in Proceedings of the 1987 Particle Accelerator Conference (Ref. 3), p. 920.

[5]W. K. Tucker et al., in Proceedings of the 1987 Particle Accelerator Conference (Ref. 3), p. 957.

[6]P. Sprangle and C. A. Kapetanakos, J. Appl. Phys. 49, 1 (1978).

[7]C. A. Kapetanakos et al., Phys. Fluids 26, 1634 (1983).

[8]N. Rostoker, Comments Plasma Phys. 6, 91 (1980).

[9]C. Roberson et al., Phys. Rev. Lett. 50, 507 (1983).

[10]C. A. Kapetanakos et al., Part. Accel. 21, 1 (1987).

[11]C. A. Kapetanakos et al., Phys. Rev. Lett. 61, 86 (1987).

[12]S. J. Marsh et al., J. Appl. Phys. 64, 6138 (1988).

[13]D. W. Kerst, Nature (London) 157, 90 (1946).

[14]P. Sprangle and C. A. Kapetanakos, Part. Accel. 18, 203 (1986).

[15]D. Chernin and P. Sprangle, Part. Accel. 12, 101 (1982).

[16]C. W. Roberson et al., Part. Accel. 17, 79 (1985).

[17]P. Sprangle (private communication).

[18]F. C. Young, IEEE Trans. Nucl. Sci. 22, 718 (1975).

Major Axis

Injection Position

Target Foil (10 μm)

Minor Axis

5172

B_θ = 1.9 kG
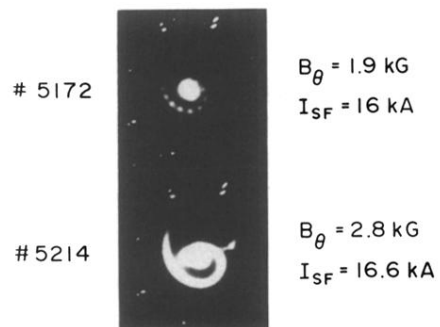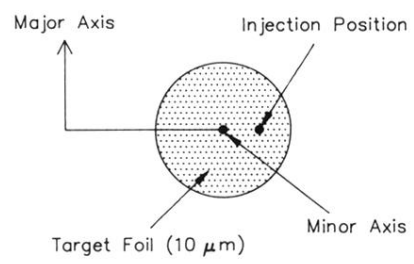
I_{SF} = 16 kA

#5214

B_θ = 2.8 kG

I_{SF} = 16.6 kA

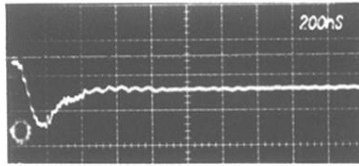FIG. 2. Open-shutter photographs of the light emitted when the beam passes a 10-μm-thick foil.

FIG. 3. Output from a Rogowski coil that is located 15° downstream of the diode. The plateau (trapped current) corresponds to 525 A.